Study of Isothermal Behaviour of Natural Tunisian Dolomite Under Controlled Pressure of Carbon Dioxide

HAYKEL GALAI*, K. NAHDI and M. TRABELSI-AYADI
LACReSNE, Faculté des Sciences de Bizerte, 7021 Zarzouna Bizerte, Tunisia
Fax: (216)(72)590566; Tel: (216)(22)069100; E-mail: hgalai@yahoo.fr

The first half decomposition of natural Tunisian dolomite sample, was investigated by thermogravimetric measurements and *in situ* X-Ray diffraction, in controlled CO_2 pressure ($20 < P_{CO_2} < 500h$ Pa) and in isothermal conditions (in the temperature range 823-1023 K). The thermograms exhibited two consecutive weight losses, corresponding to fractional conversion ranges of 0-0.2 and 0.2-1. A decelerating effect of was observed only during the second weight loss. *In situ* X-ray diffraction results indicate that crystal lattice of dolomite undergoes, during the thermal treatment, a dilatation along the c direction, then it decomposes progressively into poor crystalline MgO and a magnesian calcite $Mg_{0.052}Ca_{0.948}CO_3$. The characterization of the final product using SEM and XPS has shown that MgO could precipitate at the surface of $CaCO_3$.

Key Words: Isobaric and Isothermal thermogravimetry, Solid solution, Dolomite.

INTRODUCTION

The thermal decomposition of dolomite $CaMg(CO_3)_2$ has been the subject of numerous kinetic measurements. These studies were done on dolomites, having different chemical compositions and under experimental conditions which involved multiple parameters such as: sample weight, grain size, mechanical treatment, *etc.* The calcination conditions *e.g.*, temperature programmed or isothermal heating treatment, under static or dynamic atmospheres, isobaric decomposition in vacuum, under carbon dioxide partial pressure, inert gas or dry air flux.

The kinetic studies of reversible decomposition reactions are sensitive to the prevailing conditions. Consequently the information related to thermal decomposition of dolomite is confusing and show considerable deviations, because of the wide range of reported kinetic parameters.

The dolomite thermolysis takes place in different ways depending on partial carbon dioxide pressure (P_{CO_2}). Indeed two different decomposition paths can occur: (a) under low carbon dioxide pressure (P_{CO_2}), dolomite is directly decomposed into CaO and MgO following the reaction noted E-0:

$$CaMg(CO_3)_2 = CaO + MgO + 2CO_2 \qquad\qquad (E\text{-}0)$$

(b) under high carbon dioxide pressure, dolomite is decomposed *via* two reactions noted E-1 and E-2:

$$CaMg(CO_3)_2 = CaCO_3 + MgO + CO_2 \qquad\qquad (E\text{-}1)$$

$$CaCO_3 = CaO + CO_2 \qquad\qquad (E\text{-}2)$$

There is a controversy in the literature about the value of the limiting P_{CO_2} at which the course of dolomite decomposition switches from E-0 to E-1 and E-2. Its value varies between 5 to 200 hPa[1-4]. Spinolo and Beruto[5] noted that it is not clear if this critical pressure is a thermodynamic or kinetic parameter and if it depends or not on the temperature.

The thermal behaviour of dolomite decomposition is still under debate[6]. It is commonly thought that the first half decomposition reaction (E-1) is at the origin of the contradictory interpretations. The precise mechanism of this step is not yet established and there is still some confusion concerning its sensitivity to P_{CO_2}.

Indeed, to describe the mechanism of the first stage, E-1, many authors have proposed that solid solutions such as $CaCO_3(1\text{-}n)MgCO_3$[7,8]; $(1\text{-}x)CaCO_3 (1\text{-}y)MgO$[9,10]; $CaMg_{1\text{-}x}(CO_3)_{2\text{-}x}$[11]; $Ca_{1\text{-}x}Mg_xCO_3$[12] and $MgO\text{-}CaCO_3$[13,14] can be intermediate compounds for the formation of MgO and calcite. Other authors[15-17] consider that the decomposition of the dolomite begins with the dissociation into individual carbonates, *i.e.*, $MgCO_3$ and $CaCO_3$.

Using temperature programmed temperature, some authors[1,14,16,18] consider that the temperature of the DTG peak relative to E-1 does not depend on CO_2 pressure and other authors[2,17,19] noted an abnormal effect of on the latter peak; when P_{CO_2} decreases, the temperature of this peak begins to decrease, then increases.

Comparatively, few works are devoted to the study of the thermal decomposition of dolomite under isothermal and isobaric conditions[7,9,15,20]. In addition, the P_{CO_2} effect on isothermal and isobaric decomposition of dolomite has not yet been studied.

In present work, the main goal is to study the behaviour of the first half decomposition (step E-1) of a Tunisian dolomite under isothermal and isobaric conditions. The influence of temperature and P_{CO_2} has been pointed out. The starting and final products of the first half decomposition of dolomite were characterized with scanning electron microscopy, *in situ* X-ray diffraction, nitrogen adsorption and X-ray photoelectron spectroscopy. Finally, a reaction path for the thermal decomposition of dolomite was proposed.

EXPERIMENTAL

The symmetrical SETARAM MTB 10-8 equipped with a vertically moved furnace, thermobalance is used for the isothermal gravimetry.

At the beginning of the experiments, the furnace (heated at the temperature chosen for the experiment) is in a low position so that the sample is maintained at about 523 K during 1 h (during this step, desorption of water occurs, leading to a measured weight loss ranging between 1 to 1.5 %). Once the sample is degassed in vacuum to get rid of any air existing in the thermobalance, carbon dioxide is introduced until reaching the pressure chosen for the experiment. Calcinations are thus carried out under controlled static CO_2 atmosphere. In order to ensure the isobaric conditions even at low pressure (20 hPa), only 5 ± 1 mg of dolomite is used, the amount of CO_2 released during the reaction remaining negligible besides the starting CO_2 pressure.

Once the desired pressure around the sample is established and the signal of the mass loss is stabilized, the furnace is quickly raised up to heat the sample. Isothermal condition is thus attained after 5 min.

A thermobalance SETARAM DSC 111 was also used, in which 20 mg samples were isothermally heated under total flow rate of 2 L h^{-1}.

Similar experiments were carried out with empty crucibles in order to substract the baseline to the signals measured with the samples (but in fact the baseline signals can be neglected compared to the signals obtained with the samples).

High temperature X-ray diffraction measurements were performed with a Bruker D8-Advance diffractometer which is equipped with a heating chamber. Before each experiment, the sample chamber was purged with flowing helium, then the controlled atmosphere (20 % CO_2 - 80 % He) was established (total flow rate 8 L h^{-1}). Samples were heated rapidly (10 K s^{-1}) up to the chosen temperature.

Concerning both analysis (thermogravimetry and *in situ* XRD), similar experimental conditions were fixed ($823 < T < 1023$ K and $20 < P_{CO_2} < 500$ hPa), in order to correlate the evolution of the various phases with the weight losses observed by TGA.

The scanning electron microscope (SEM) studies were performed on the Jeol JSM-6500 microscope, wherein the surface of the sample was coated with a thin gold conductive film. The excitation voltage used was 15 kV. ESCA electron spectrometer with AlKα (1486.6 eV) anode was used to characterize the surfaces of the sample.

The composition of the dolomite originating from Menzel Mhiri (center of Tunisia) used in this study has been determined by fluorescence X to be $Ca_{0.498} Mg_{0.502} CO_3$. Considering the water and impurities contents in the powder, the fraction of dolomite has been determined to be 92.5 % (Table-1).

4234 Galai *et al.*
Asian J. Chem.

TABLE-1
FLUORESCENCE X ANALYSIS OF THE STARTING MATERIAL

Species	SiO_2	TiO_2	Al_2O_3	FeO_3	MnO	MgO	CaO	K_2O	P_2O_5	Water loss*
Content (%)	4.163	0.044	0.675	0.354	0.007	21.531	29.696	0.066	0.583	1.5-2.5
Theoretical composition						21.830	30.410			

*Water loss quantity was determined by coupling thermogravimetry and mass spectrometry.

This sample was first hand ground in an agate mortar and then dry-sieved. The fraction with particle dimensions in the range of 100-120 µm was used. A scanning electron microscopy micrograph of this powder is shown in Fig. 1. It indicates that grains have a cubic shape approximately (Fig. 1a) and are composed of aggregated needle-shaped elementary particles (Fig. 1b).
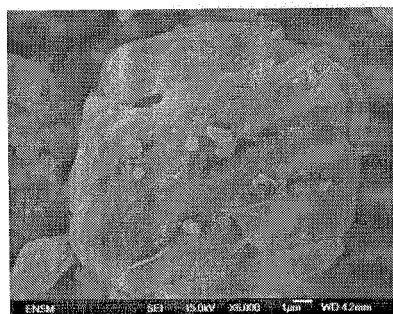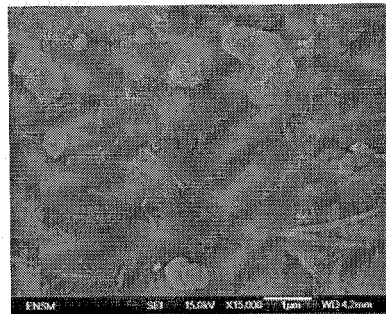
(a)   (b)

Fig. 1. SEM micrographs of the starting sample

The specific surface area of the starting material was 7 m^2 g^{-1} (measured by nitrogen adsorption at 77 K, using BET method, in a Micrometrics Asap 2000 analyzer).

RESULTS AND DISCUSSION

Several programmed temperature experiments (2°C min^{-1}) at different CO_2 pressure were carried out in order to determine experimentally the threshold pressure, under which the reaction E-0 or E-1and E-2 occurs.

Fig. 2 shows TG curves recorded under P_{CO_2} ranging between 10-100 hPa (static atmosphere). It indicates that dolomite decomposes into CaO and MgO in two stages (E-1 and E-2) when P_{CO_2} is higher than 35 hPa (this pressure is in agreement with the data reported in the literature[3,9].

Fig. 3 shows isothermal TG curve (DSC 111) recorded at 990 K. In the part A-C the atmosphere was a CO_2-He mixture, then dolomite decomposed into $CaCO_3$ and MgO. When the mass loss was stabilized (point C, Dm = -23 %), the atmosphere was switched to pure He, which led to decarbonation of $CaCO_3$ into CaO (Dm = -43 %). However XRD analysis (Fig. 4) of the sample obtained on D, indicated the presence of traces of spurrite ($Ca_5Si_2O_8CO_3$). The latter phase decomposed at 1300 K. The total weight loss 45.5 % at 1500 K is close to expected one 46.1 %

Taking into account the water loss corresponding to the part A-B (2%), the weight losses B-C (21 %) and C-D (20 %) can be attributed to the first and second stages of dolomite decomposition (E-1 and E-2).

As the given dolomite is stoichiometric (DRX-chemical analysis), it is expected to have 22 % as CO_2 weight loss per each stage (E-1 and E-2). This deviation can be explained by the fact that the identified products in D and C are spurrite and magnesian calcite, respectively in which the Mg content has been evaluated to be around 5.2 %, as explained in the following.
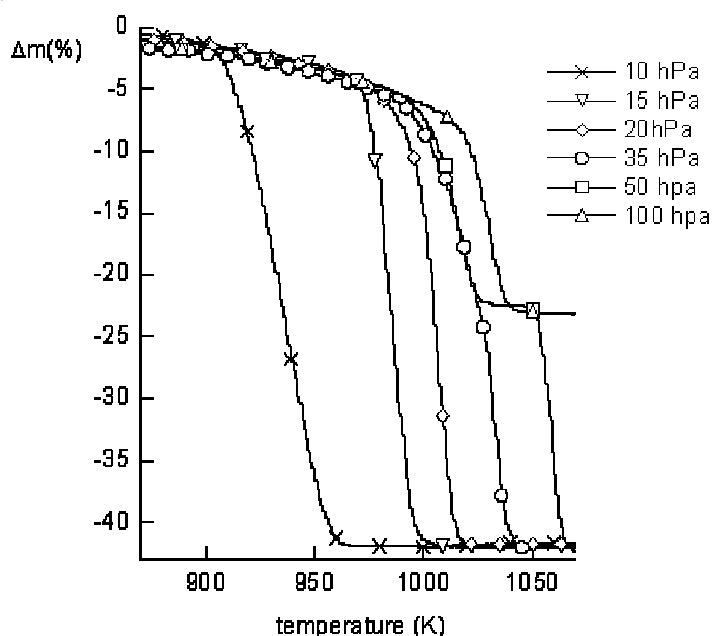
Fig. 2.   TG curves of dolomite heated (2°C min⁻¹) under various (static atmosphere)
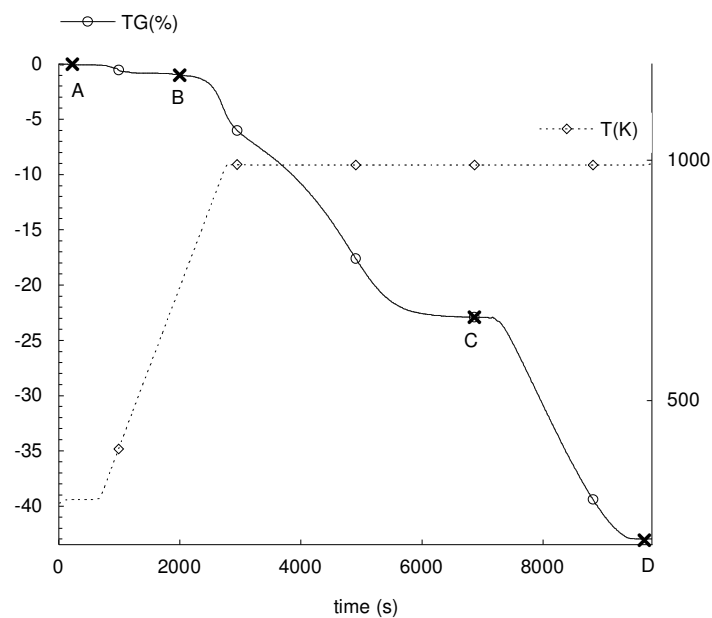
Fig. 3. Isothermal TG curve of dolomite (flowing atmosphere) : decomposition at 990 K showing two steps E-1 (He (95 %) - CO_2 (5 %)) and E-2 (100 % He)
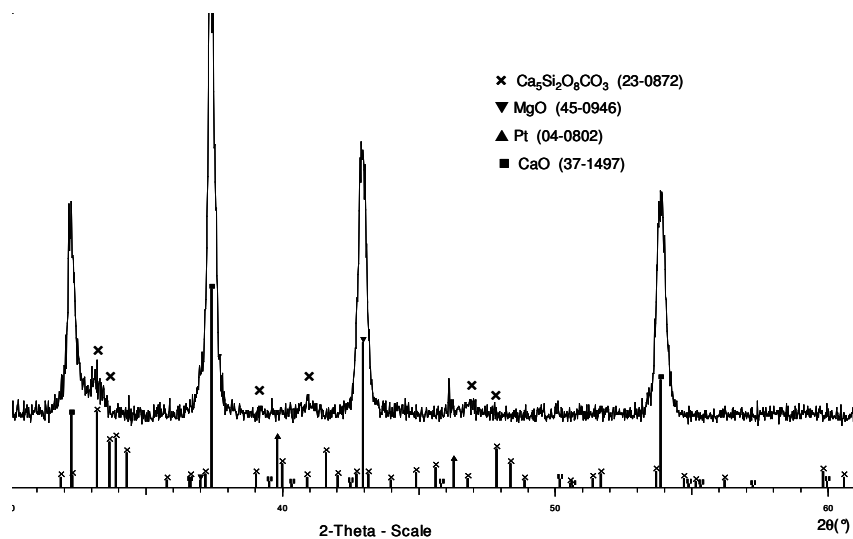
Fig. 4. Diffractogramm of dolomite obtained after heating at 990K (after E1 and E2 steps)

Fig. 5 shows the typical shape of the weight loss (% TG) and the rate $\dfrac{dm}{dt}$ (%/h) *vs.* time obtained for the first half decomposition of dolomite. These curves are obtained at 923 K under $P_{CO_2} = 20$ hPa. They indicate that the rate of the transformation increased at the beginning, then it decreased around a weight loss of 5.5 % and increased again at 9.5 %. The whole transformation lasted 23 h.

The shape of the TG curve leads us to assume that the first half decomposition E-1 of dolomite occurs in two steps, an intermediate phase may be formed.

The effect of temperature and P_{CO_2} on the reaction rate (formation of $CaCO_3$ and MgO) was studied by means of isothermal gravimetry under controlled P_{CO_2}.

A series of isothermal experiments at various temperatures, under $P_{CO_2} = 20$ hPa, were carried out in static conditions, typical curves are given in Figs. 6a and 6b. In all experiments, the final weight loss is about 22 %, which is in agreement with the value reported in Fig. 3, since in static conditions, water desorption (1 %) occurs before the beginning of the experiments. Moreover water loss (1 %) continued up to 650 K.
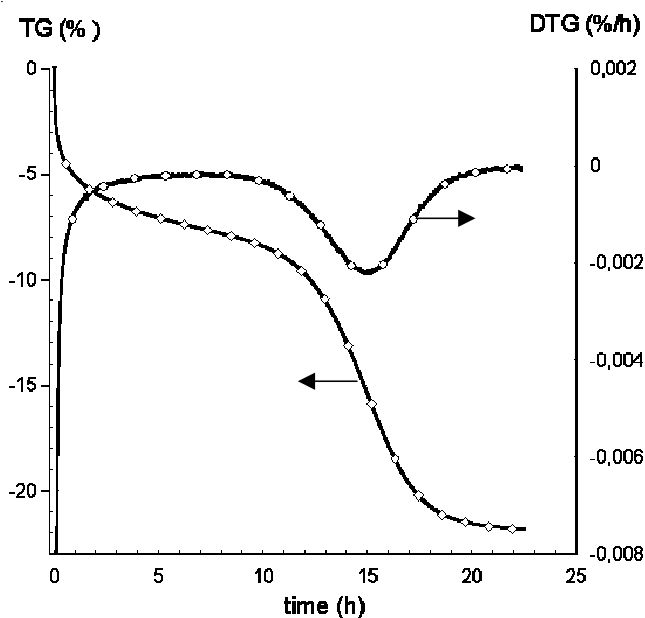
Fig. 5. Isothermal TG curve giving the weight gain (%) and the rate (%/h) *vs.* time, at 923K under $P_{CO_2} = 20$ hPa (static atmosphere)
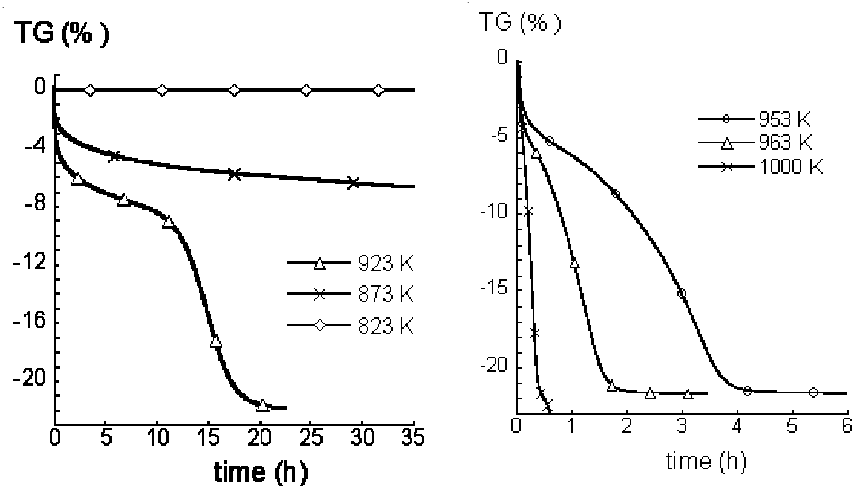
Fig. 6. Kinetic curves $\Delta m(t)$ under P_{CO_2} = 20 hPa, at 823-1000 K
(static atmosphere)

It can be noted that at 823 K the decomposition does not occur, whereas above 1000 K, the full decomposition of dolomite (E-0) directly occurs. On the other hand, between 953 and 963 K, the kinetic curves exhibit two parts; a first weight loss up to about 5.5 %, then a sigmoïdal part up to the end. This sigmoïdal part has not been observed even after 3 d at 873 K (Fig. 6b).

Curves obtained at different P_{CO_2} are shown in Fig. 7. The CO_2 pressure has no effect on the first part of the kinetic curves (Δm = 5.5 %) and
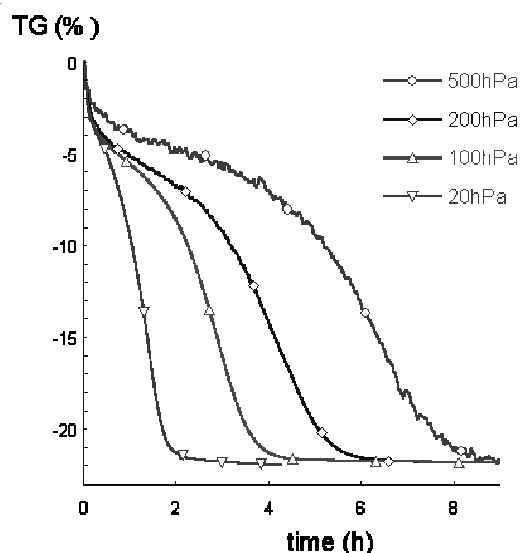
Fig. 7. Kinetic curves $Dm(t)$ at 963 K under P_{CO_2} = 20, 100, 200 and 500 hPa (static atmosphere)

has an inhibiting effect on the reaction rate when $\Delta m \geq 5.5$ %. Depending on the CO_2 pressure, from 20 to 500 hPa, the reaction time ranges between 2 and 10 h.

Finally, the shape of both sets of isothermal and isobaric curves (Figs. 3, 6 and 7) is similar and it reveals that the decomposition of dolomite (E-1) does not proceed in the same way for 0-5.5 and 5.5-22 % conversion ranges. A two step decomposition into $CaCO_3$ and MgO may thus be considered, involving the formation of an intermediate phase corresponding to $\Delta m \approx 5.5$ % (when $T \leq 963$ K and $20 < P_{CO_2} < 500$ hPa).

In order to identify the intermediate and final products of the half decomposition of dolomite, *in situ* XRD experiments have been performed.

An internal standard (Si) was thoroughly prepared by mixing 5 % by weight of silicium with the starting material. XRD powder patterns were recorded during the heating of the sample at 953 K under $P_{CO_2} = 200$ hPa. Under these conditions, the dolomite half decomposition appeared to be completed after 12 h.

Fig. 8 shows the XRD patterns of the starting dolomite (a) and its decomposition products at 953 K recorded at various times 0 h (b) (*i.e.* as soon as the temperature reached 953 K), 6 h (c), 12 h (d). The pattern (e) is recorded at room temperature after decomposition. Each diffractogram lasted 3 h. As a reference, the reflections positions of the following phases are shown (★, Si, JCPDS : 27-1402); (✦, Pt, JCPDS : 04-0802); (□, dolomite, JCPDS : 36-0426); (▽, $CaCO_3$, JCPDS : 47-1743); (▼, MgO, JCPDS : 75-1525). The platinum peaks are due to the sample holder, it can be noticed that they are not clearly observed in diffractograms (c) to (e), due to the appearance of calcite, which peaks are very close to the platinum ones.

As it can be observed on diffractogram (b) at 953 K, the dolomite reflections are displaced non-systematically towards low angles. The same displacement was observed at 773 K, temperature too low to observe any transformation of the sample. Consequently the peak shift is only due to temperature most probably (this well-known temperature effect also appears clearly on some calcite and platinum peaks, which positions are slightly different at high temperature [diffractograms (b) to (d)] and at room temperature [diffractogram (e)].

Using EVA refinement, software developed by SOCABIM, the peaks (❖) belong to diffractogram (b) have been attributed to a transistory dolomite with cell parameters a = 4.809 Å and c = 16.28 Å.

On the other hand, examination of the first pattern recorded at 953 K (b) reveals the emergence of a peak between 42 and 43° 2θ which can be ascribed to magnesium oxide. Moreover it can be noted that MgO grows faster than $CaCO_3$, since no calcium carbonate peak was observed on this diffractogram (b).
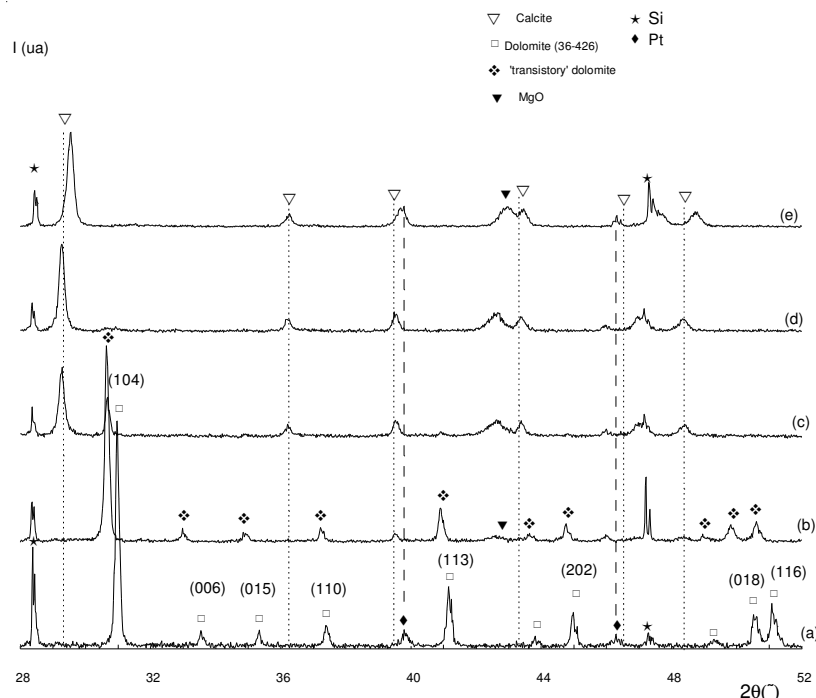
Fig. 8. *In situ* XRD patterns of dolomite: starting sample (a), calcined at 953 K in 200 hPa of CO_2, from 0h (b), 6h (c), 12h (d) and after cooling at room temperature (e). The peaks shift in (b) is only due to the temperature increase. The vertical dashed lines correspond to the JCPDS files: 04-0802 for Pt and 47-1743 for $CaCO_3$

Considering the kinetic curves represented on Figs. 6 and 7, it can be concluded that the diffraction pattern (b) (Fig. 8) corresponds to a dolomite which is partially transformed, up to about 5.5 % of weight loss, even though there is no evidence for a structure change on XRD data.

As far as the reaction progressed, the peaks related to the transistory dolomite, MgO and calcite kept a constant position. The characterization of the end product [Fig. 8, pattern (e)] revealed that the phase for which the major peak was at 29.4° (pseudo-calcite) was well crystallized. Its diffraction peaks could not be well indexed by comparing them with the data files of calcite but it turned out that among the listed phases in the data base, a magnesian calcite ($Ca_{0.936}$ $Mg_{0.064}$ CO_3, JCPDS 86-2335) was the most appropriate one (Fig. 9).

The formation of a solid solution of magnesium in calcite has already been suggested at moderate temperature[9], even if the Mg content was not evaluated.

By fitting the reflections of the magnesium calcite obtained at 953 K with a Rietveld refinement (using Winploter software), its lattice parameters were determined: a = b = 4.954 Å and c = 17.04 Å. The observed,
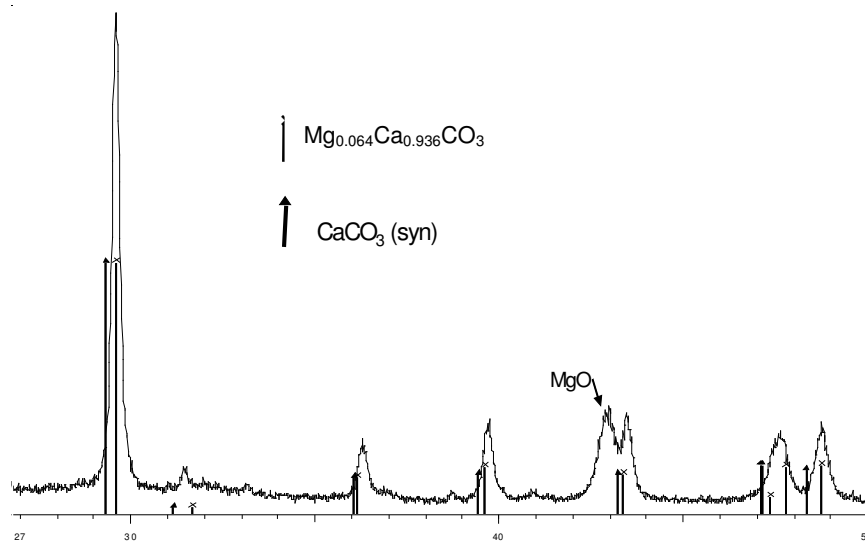
Fig. 9. XRD *in situ* pattern of dolomite, calcined at 953 K during 12 h. The vertical line indicated the expected peaks of $Ca_{0.936}Mg_{0064}CO_3$ (×, JCPDS n°: 86-2335) and calcite (▲, JCPDS n°: 47-1743)

calculated and difference profiles of the dolomite decomposition product are given in Fig. 10.

The lattice volume of the obtained phase is then 362.45 Å³. This value is smaller than that of natural calcite (367.76 Å³), most probably due to the presence of Mg^{2+} in the crystal structure.
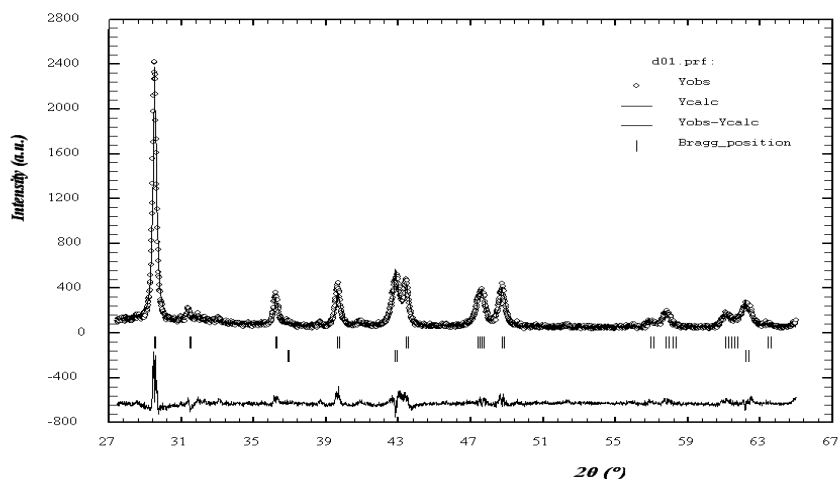
Fig. 10. Observed (o), calculated (-) and difference (bottom) profiles for the Rietveld refinement of dolomite decomposition product

Using the JCPDS data, the cell volume values of the calcite and different natural magnesian calcites $Mg_xCa_{1-x}CO_3$ (x = 0.064, 0.10 and 0.129, JCPDS 86-2335; 71-1663 and 86-2336) are presented in Fig. 11, which shows the linear relationship between the cell volume and the Mg content. From this curve, the Mg content in present magnesian calcite could be evaluated around 5.2 %.
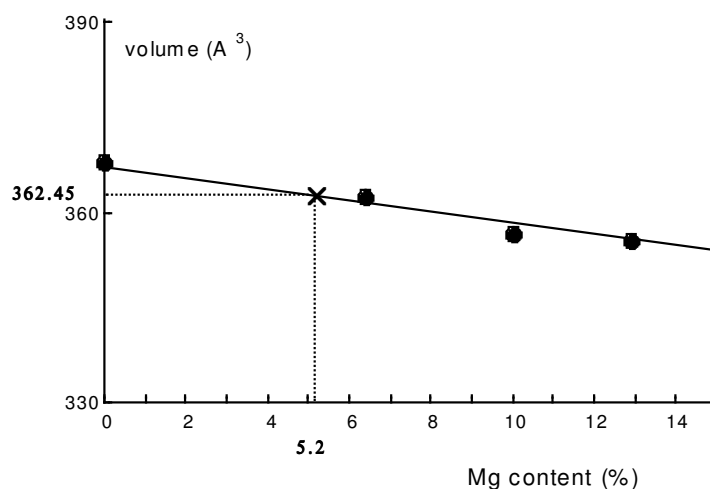
Fig. 11. Variation of the cell volume of calcite and different magnesian calcites, with increasing Mg content. The straight line was obtained by least-squares analysis (R = 0.99)

SEM micrography, XPS analysis and specific surface area

Scanning electron micrographs of samples calcined up to various values of weight loss were obtained (Fig. 12). It can be observed that at Δm = 5.5 % (Fig. 12b) the aggregated particles kept their external shape but became less compact. As the decomposition conversion is increased, a significant change of the morphology occurred: fine spherical particles appeared on particle surface (Figs. 12c and 12d).

(a)	(b)

| (c) | (d) |
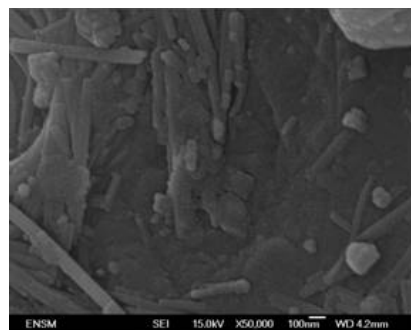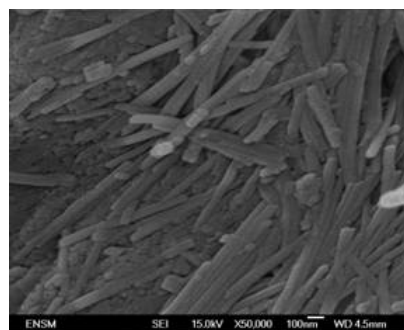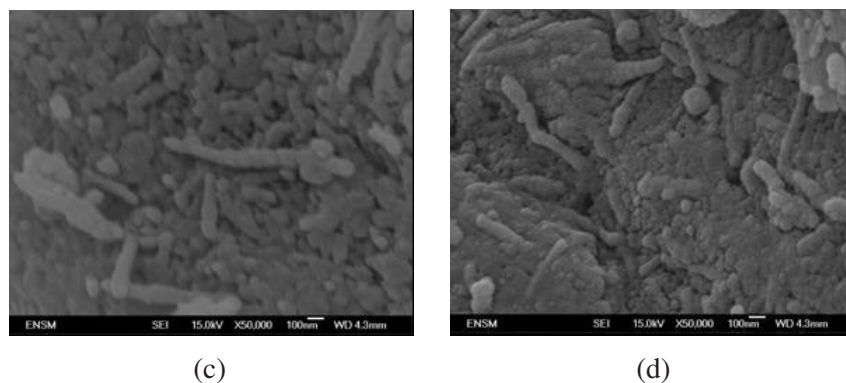
Fig. 12. SEM micrographs of undecomposed dolomite (a), dolomite decomposed up to $\Delta m = 5.5$ % (b); $\Delta m = 16$ % (c); final product (d)

XPS analysis was carried out on the starting dolomite powder and the final product of its half decomposition. Mg/Ca ratio was determined from the areas of Mg 2p and Ca 2p peaks. It provides the information that the Mg/Ca ratio increased from 0.24 to 0.39.

The specific surface area of the sample obtained at $\Delta m = 5.5$ % and of the final product was 7.2 and 10 $m^2\ g^{-1}$, respectively; such an increase is in agreement with the SEM observations.

Conclusion

The general reaction path for the first half thermal decomposition of Tunisian dolomite in controlled CO_2 pressure ($20 < P_{CO_2} < 500hPa$) can be written as follow:

$$MgCa(CO_3)_2 = \frac{1}{1-x}Ca_{1-x}Mg_xCO_3 + \frac{1-2x}{1-x}MgO + \frac{1-2x}{1-x}CO_2 \qquad (2)$$
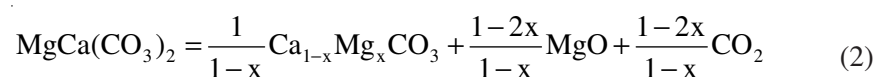
in which x is equal to 0.052.

Even *in situ* XRD did not show clearly any structure change of dolomite due to the formation of a stable intermediate phase during this reaction, it can be assumed that this natural dolomite first half decomposition under these experimental conditions proceeds in two steps, corresponding to the conversion ranges 0-0.2 ($\Delta m < 5.5$ %) and 0.2-1 ($\Delta m > 5.5$ %) since the effect of temperature and CO_2 pressure in the latter domain (Figs. 6 and 7) on the kinetic curves was not the same.

Taking into account XPS results, the fine particle observed on the surface of final product could be the MgO phase which precipitated at the external surface of calcium carbonate.

REFERENCES

1. R.A.W. Haul and D. Heystek, *Am. Mineral.*, **37**, 166 (1952).
2. W.R. Bandi and G. Krapf, *Thermochim. Acta*, **14**, 221 (1976).
3. C.H. Bamford and C.F.H. Tipper, Chemical Kinetics, Elsevier, Amsterdam (1980).
4. H.G. Wiedmann and G. Bayer, *Thermochim. Acta*, **121**, 479 (1987).
5. G. Spinolo and D. Beruto, *J. Chem. Soc. Faraday Trans.*, **78**, 2631 (1982).
6. M. Samtani, D. Dollimore, F.W. Wilburn and K. Alexander, *Thermochim. Acta*, **367-368**, 285 (2001).
7. H. Hashimoto, E. Komaki and F. Hayashi, *Solid State Chem.*, **33**, 181 (1980).
8. D. Beruto and A.W. J. Searcy, *J. Chem. Soc. Faraday Trans. I*, **70**, 2145 (1974).
9. D. Beruto, R. Vecchiattini and M. Giordani, *Thermochim. Acta*, **405**, 183 (2003).
10. D. Beruto, R. Vecchiattini and M. Giordani, *Thermochim. Acta*, **404**, 25 (2003).
11. A.H. DeAza, M.A. Rodríguez, J.L. Rodríguez, S. DeAza, P. Pena, P. Convert, T. Hansen and X. Turrillas, *J. Am. Ceram. Soc.*, **85**, 881 (2002).
12. A.W. Searcy and D. Beruto, *J. Phys. Chem.*, **82**, 163 (1978).
13. A. Ersoy-Meriçboyu and S. Küçükbayrak, *Thermochim. Acta*, **232**, 225 (1994).
14. R. Martensson and I. Bjerle, *Chem. Eng. Tech.*, **19**, 364 (1996).
15. R.M. McIntosh, J.H. Sharp and F.W. Wilburn, *Thermochim. Acta*, **165**, 281 (1990).
16. J.S. Dennis and N. Hayhurst, *Chem. Eng. Sci.*, **42**, 2361 (1987).
17. D. Dollimore, J.G. Dunn, Y.F. Lee and B.M. Penrod, *Thermochim. Acta*, **237**, 125 (1994).
18. R. Ozao, M. Ochiai, A. Yamazaki and R. Otsuka, *Thermochim. Acta*, **183**, 183 (1991).
19. R. Otsuka, *Thermochim. Acta*, **100**, 69 (1986).
20. P.G. Caceres and E.K. Attiogbe, *Miner. Eng.*, **10**, 1165 (1997).